arXiv:hep-ph/0511032v1 3 Nov 2005

SOFFER BOUND AND TRANSVERSE SPIN DENSITIES FROM LATTICE QCD [*]

M. DIEHL[1], M. GÖCKELER[2], PH. HÄGLER[3], R. HORSLEY[4],
D. PLEITER[5], P.E.L. RAKOW[6], A. SCHÄFER[2], G. SCHIERHOLZ[1,5] AND
J.M. ZANOTTI[4]

[1] *Deutsches Elektron-Synchrotron DESY, 22603 Hamburg, Germany*
[2] *Institut für Theoretische Physik*
Universität Regensburg, 93040 Regensburg, Germany
[3] *Institut für Theoretische Physik T39, Physik-Department der TU München,*
James-Franck-Straße, D-85747 Garching, Germany
[4] *School of Physics, University of Edinburgh, Edinburgh EH9 3JZ, UK*
[5] *John von Neumann-Institut für Computing NIC / DESY*
15738 Zeuthen, Germany
[6] *Theoretical Physics Division, Dep. of Math. Sciences, University of Liverpool,*
Liverpool L69 3BX, UK

QCDSF/UKQCD COLLABORATIONS

Generalized transversity distributions encode essential information on the internal structure of hadrons related to transversely polarized quarks. Lattice QCD allows us to compute the lowest moments of these tensor generalized parton distributions. In this talk, we discuss a first lattice study of the Soffer bound and show preliminary results for transverse spin densities of quarks in the nucleon.

1. Introduction

Generalized parton distributions (GPDs) [1, 2] are an ideal tool to study many fundamental facets of hadron structure in terms of quarks and gluons. One key point is the relation of GPDs to (orbital) angular momentum, which plays a central role for the nucleon spin sum rule [3]. Moreover, GPDs allow us to investigate the nontrivial interplay of longitudinal momentum and transverse coordinate space degrees of freedom [4–6]. In this contribution, we will focus our attention on the recently observed correlation of transverse quark spin and impact parameter which shows up in transverse

---

[*]Preprint Edinburgh 2005/19, DESY 05-218, LTH 680

2

spin densities of quarks in the nucleon [7]. It turns out that these correlations in the transverse plane are governed by quark helicity flip (or tensor) GPDs [8]. As in the case of the unpolarized and the polarized GPDs [2], they are defined via the parametrization of an off-forward nucleon matrix element of a bilocal quark operator as follows

$$\langle P',\Lambda'|\int_{-\infty}^{\infty}\frac{d\lambda}{4\pi}e^{i\lambda x}\bar{q}\left(-\frac{\lambda}{2}n\right)n_\mu\sigma^{\mu\nu}\gamma_5\mathcal{U}q\left(\frac{\lambda}{2}n\right)|P,\Lambda\rangle=\overline{u}(P',\Lambda')n_\mu\Bigg\{$$

$$\sigma^{\mu\nu}\gamma_5\left(H_T(x,\xi,t)-\frac{t}{2m^2}\widetilde{H}_T(x,\xi,t)\right)+\frac{\epsilon^{\mu\nu\alpha\beta}\Delta_\alpha\gamma_\beta}{2m}\overline{E}_T(x,\xi,t)$$

$$+\frac{\Delta^{[\mu}\sigma^{\nu]\alpha}\gamma_5\Delta_\alpha}{2m^2}\widetilde{H}_T(x,\xi,t)+\frac{\epsilon^{\mu\nu\alpha\beta}\overline{P}_\alpha\gamma_\beta}{m}\widetilde{E}_T(x,\xi,t)\Bigg\}u(P,\Lambda)\,, \qquad (1)$$

where $f^{[\mu\nu]}=f^{\mu\nu}-f^{\nu\mu}$, $\Delta=P'-P$ is the momentum transfer with $t=\Delta^2$, $\overline{P}=(P'+P)/2$, and $\xi=-n\cdot\Delta/2$ defines the longitudinal momentum transfer with the light-like vector n. The Wilson line ensuring gauge invariance of the bilocal operator is denoted by $\mathcal{U}$. Our parametrization in Eq. (1) in terms of the four independent tensor GPDs slightly differs from the literature [7,8] where a function E_T instead of $\overline{E}_T$ has been used. However, in [7, 9] it has been noted that E_T typically appears in linear combination with the tensor GPD $\widetilde{H}_T$. It is therefore reasonable to adopt a new notation and consider $\overline{E}_T=E_T+2\widetilde{H}_T$ and $\widetilde{H}_T$ as fundamental quantities.

One prominent feature of GPDs is that they reproduce the well known parton distributions in the forward limit, $\Delta=0$, and that their integral over the momentum fraction x leads directly to form factors. For this reason, the GPD $H_T(x,\xi,t)$ is called generalized transversity, since for vanishing momentum transfer it is equal to the transversity parton distribution, $H_T(x,0,0)=\delta q(x)=h_1(x)$ for $x>0$ and $H_T(x,0,0)=-\delta\bar{q}(-x)=-\bar{h}_1(-x)$ for $x<0$. On the other hand, integrating $H_T(x,\xi,t)$ over x gives the tensor form factor:

$$\int_{-1}^{1}dxH_T(x,\xi,t)=g_T(t). \qquad (2)$$

Another feature of GPDs important for our investigations below is their interpretation as densities in the transverse plane for $\xi=0$ [4]. To give an example, it has been shown that the impact parameter dependent quark distribution for the quark GPD H_q,

$$q(x,b_\perp)\equiv\int\frac{d^2\Delta_\perp}{(2\pi)^2}e^{-ib_\perp\cdot\Delta_\perp}H_q(x,\xi=0,t=-\Delta_\perp^2), \qquad (3)$$

has the interpretation of a probability density for unpolarized quarks of flavor q with longitudinal momentum fraction x and transverse position $b_\perp = (b_x, b_y)$ relative to the center of momentum in a nucleon.

In order to facilitate the computation of the tensor GPDs in lattice QCD, we first transform the LHS of Eq. (1) to Mellin space by forming the integral $\int_{-1}^{1} dx\, x^{n-1} \cdots$. This results in nucleon matrix elements of towers of local tensor operators

$$\mathcal{O}_T^{\mu\nu\mu_1\cdots\mu_{n-1}}(0) = \bar{q}(0) i\sigma^{\mu\{\nu}\gamma_5 i\overset{\leftrightarrow}{D}^{\mu_1} \ldots i\overset{\leftrightarrow}{D}^{\mu_{n-1}\}} q(0) , \qquad (4)$$

which are parametrized in terms of tensor generalized form factors (GFFs) A_{Tni}, $\overline{B}_{Tni}$, $\widetilde{A}_{Tni}$ and $\widetilde{B}_{Tni}$. Here, $\overset{\leftrightarrow}{D} = \frac{1}{2}(\vec{D} - \overset{\leftarrow}{D})$ and $\{\cdots\}$ indicates symmetrization of indices and subtraction of traces.[a] For $n = 1$, we have [8, 10]

$$\langle P'\Lambda'| \bar{q}(0) i\sigma^{\mu\nu}\gamma_5 q(0) |P\Lambda\rangle = \overline{u}(P', \Lambda') \Bigg\{ \sigma^{\mu\nu}\gamma_5 \left(A_{T10}(t) - \frac{t}{2m^2}\widetilde{A}_{T10}(t) \right)$$

$$+ \frac{\epsilon^{\mu\nu\alpha\beta}\Delta_\alpha\gamma_\beta}{2m}\overline{B}_{T10}(t) + \frac{\Delta^{[\mu}\sigma^{\nu]\alpha}\gamma_5\Delta_\alpha]}{2m^2}\widetilde{A}_{T10}(t) \Bigg\} u(P, \Lambda) . \qquad (5)$$

The relation of the lowest moment of the tensor GPDs to the GFFs is simple and given by

$$H_T^{n=1}(\xi, t) = A_{T10}(t) = g_T(t), \qquad \widetilde{H}_T^{n=1}(\xi, t) = \widetilde{A}_{T10}(t)$$
$$\overline{E}_T^{n=1}(\xi, t) = \overline{B}_{T10}(t), \qquad \widetilde{E}_T^{n=1}(\xi, t) = \widetilde{B}_{T10}(t) = 0 ,$$

where $H_T^n(\xi, t) \equiv \int_{-1}^{1} dx\, x^{n-1} H_T(x, \xi, t)$. The general parametrization in terms of GFFs and their relations to the moments of the GPDs for $n \geq 1$ can be found in [10, 11].

The calculation of moments of GPDs in lattice QCD follows standard methods, which have been described in detail in the literature [12–14]. In the following, we therefore give only an outline of the procedure we use to extract the GFFs. First, nucleon matrix elements in the form of two- and three-point functions are computed on an Euclidean space-time lattice. The typical suppression of the matrix elements by exponential factors $\exp(-\tau E)$ in the Euclidean time τ and the energy E is cancelled out by constructing an appropriate ratio $R(\tau)$ of three- to two-point functions, which is averaged over the plateau-region $R(\tau_{\text{plat.}}) \approx \text{const}$. The averaged ratio is then renormalized and equated with the continuum parametrization of the corresponding nucleon matrix element, e.g. Eq. (5), for all contributing

---

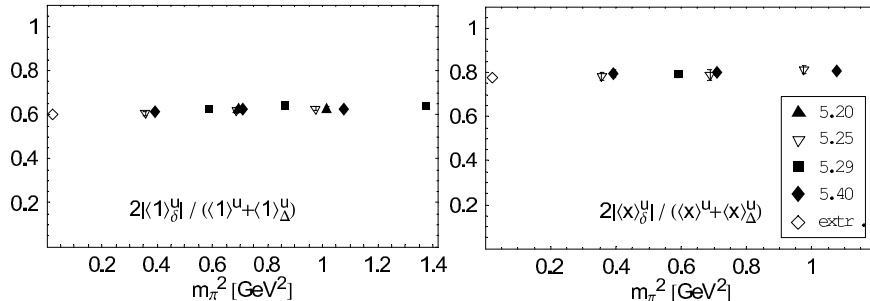[a]The Mellin-moment index n used in this work differs from the n in [10] by one.

4

Figure 1. Lattice results for the lowest two moments of the Soffer bound for up-quarks.

index (μ, ν) and momentum (P, P') combinations. This leads to an overdetermined set of linear equations which is solved to extract the GFFs. The statistical error on the GFFs is obtained from a jackknife analysis. Our results have been non-perturbative renormalized [15] and transformed to the $\overline{\text{MS}}$ scheme at a scale of 4 GeV^2.

The lattice results to be discussed below have been obtained from simulations with $n_f = 2$ flavors of dynamical non-perturbatively $\mathcal{O}(a)$ improved Wilson fermions and Wilson glue. There are 12 datasets available consisting of four different couplings $\beta = 5.20, 5.25, 5.29, 5.40$ with three different $\kappa = \kappa_{\text{sea}}$ values per β. The pion masses of our calculation vary from 550 to 1000 MeV, and the lattice spacings and spatial volumes vary between 0.07-0.11 fm and $(1.4\text{-}2.0 \text{ fm})^3$ respectively. Our calculation does not include the computationally demanding disconnected contributions. We expect, however, that they are small for the tensor GFFs [14]. More details of the simulation can be found in [14, 16, 17].

2. Lattice study of the Soffer bound

In this section, we investigate the Soffer bound [18]

$$|\delta q(x)| \leq \frac{1}{2}\Big(q(x) + \Delta q(x)\Big) \; , \tag{6}$$

which holds exactly only for quark and anti-quark distributions separately. For discussion of its validity, see e.g. [19] and section 3.12.3 of [2]. For a lattice study of the Soffer bound, we take Mellin moments of Eq. (6) and consider the "Soffer-ratio"

$$S^n = \frac{2\left|\langle x^{n-1}\rangle_\delta\right|}{\langle x^{n-1}\rangle + \langle x^{n-1}\rangle_\Delta} \; , \qquad n = 1, 2, \dots , \tag{7}$$

where $\langle x^{n-1}\rangle = \int_{-1}^{1} dx\, x^{n-1} q(x)$. At this point it is important to note that Mellin moments of distribution functions give always sums/differences of moments of quark and anti-quark distributions, e.g. $\langle x^{n-1}\rangle = \langle x^{n-1}\rangle_q + (-1)^n \langle x^{n-1}\rangle_{\bar{q}}$. Therefore, the ratio S^n in Eq. (7) is not necessarily smaller than one. Experience shows that contributions from anti-quarks are negligible in our calculation. In Fig. (1) we show our results for the ratio (7) versus the pion mass for up-quarks (similar results for down-quarks can be found in [14]). The fact that the ratio is consistently below one for the lowest two moments of the up and the down quarks strongly suggests that the Soffer bound is satisfied in our lattice calculation. The lattice results show almost no dependence on the pion mass due to cancellations of the pion mass dependence of the individual distribution functions in the ratio (7). Linear chiral extrapolation in m_π^2 leads to the following predictions for the ratios at the physical pion mass

$$
\begin{array}{lll}
\text{up-quarks} & : & S^{n=1} = 0.60\pm.01, \ S^{n=2} = 0.78\pm.01 \\
\text{down-quarks} & : & S^{n=1} = 0.57\pm.02, \ S^{n=2} = 0.73\pm.05\,.
\end{array}
\tag{8}
$$

3. Lattice results for the lowest moment of the transverse spin density

We now turn our attention to a discussion of our lattice results for the density of transversely polarized quarks in the nucleon. The lowest moment of the quark transverse spin density is given by [7]

$$
\langle P^+, R_\perp = 0, S_\perp |\, \frac{1}{2}\overline{q}(b_\perp)\big[\gamma^+ - s_\perp^j i\sigma^{+j}\gamma_5\big]q(b_\perp)\,|P^+, R_\perp = 0, S_\perp\rangle =
$$
$$
\frac{1}{2}\left\{ A_{10}(b_\perp) + s_\perp^i S_\perp^i \left(A_{T10}(b_\perp) - \frac{1}{4m^2}\Delta_{b_\perp}\widetilde{A}_{T10}(b_\perp) \right) \right.
$$
$$
+ \frac{b_\perp^j \epsilon^{ji}}{m}\left(S_\perp^i B_{10}'(b_\perp) + s_\perp^i \overline{B}_{T10}'(b_\perp) \right)
$$
$$
\left. + s_\perp^i (2b_\perp^i b_\perp^j - b_\perp^2 \delta^{ij})S_\perp^j \frac{1}{m^2}\widetilde{A}_{T10}''(b_\perp) \right\}.
\tag{9}
$$

The transversity states

$$
|P^+, R_\perp = 0, S_\perp\rangle = \frac{1}{\sqrt{2}}\Big(|P^+, R_\perp = 0, \Lambda = +\rangle + e^{i\chi}|P^+, R_\perp = 0, \Lambda = -\rangle \Big)
\tag{10}
$$

describe a nucleon with longitudinal momentum $P^+ = (P^0 + P^3)/\sqrt{2}$ which is localized in the transverse plane at $R_\perp = 0$ and has transverse spin $S_\perp = (\cos\chi, \sin\chi)$. The impact parameter dependent GFFs in Eq. (9) are
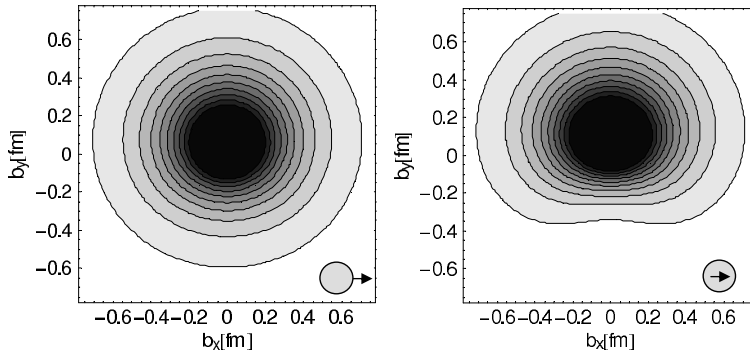
6

Figure 2. Densities of up-quarks in the nucleon. The nucleon and quark spins are oriented in the transverse plane as indicated, where the inner arrow represent the quark and the outer arrow the nucleon spin. A missing arrow represents the unpolarized case.

just the Fourier-transforms of the momentum space GFFs at $\xi = 0$, as in Eq. (3). The derivatives in Eq. (9) are defined by $f'(b_\perp) \equiv \partial_{b_\perp^2} f(b_\perp)$ and $\Delta_{b_\perp} f(b_\perp) \equiv 4\partial_{b_\perp^2} \left(b_\perp^2 \partial_{b_\perp^2} \right) f(b_\perp)$.

Since momenta are discretized on a finite lattice, we obtain the GFFs only for a limited number of different values of the momentum transfer squared t. We have in general 16 t-values available per dataset in a range of $0 \leq t < 4$ GeV^2. To facilitate the Fourier transformation to impact parameter space, we parametrize the GFFs using a p-pole ansatz

$$F(t) = \frac{F(0)}{\left(1 - t/m_p^2 \right)^p} \ , \tag{11}$$

where the parameters $F(0)$, m_p and p for the individual GFFs are fixed by a fit to the lattice results. The ansatz in Eq. (11) is then Fourier transformed in order to get the GFFs as functions of the impact parameter $b_\perp$. Details of the p-pole parametrization and numerical results for the parameters will be given in a separate publication [20]. Here we only note that the values for the power p we are using for the different GFFs lead to a regular behavior of the transverse spin density in the limit $b_\perp \to 0$, as discussed in [7]. In Figs.(2,3) we show preliminary results for the lowest moment of transverse spin densities of quarks in the nucleon for up quarks. We note that the plots do not exactly show probability densities because the lowest moment corresponds to the difference of quark and anti-quark densities. The densities are however strictly positive for all $b_\perp$, indicating that the contributions from anti-quarks are small. On the LHS of Fig.(2),
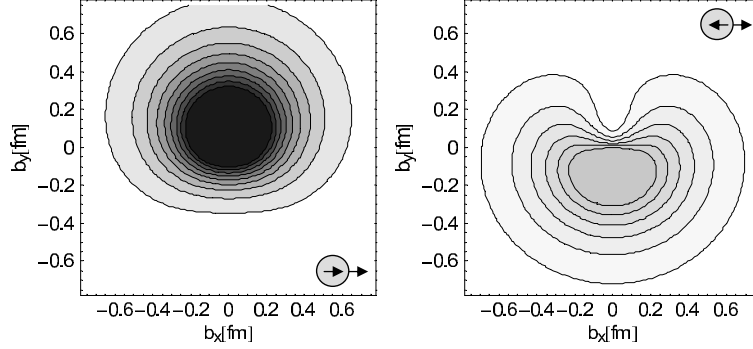
Figure 3.   Up-quark densities. Symbols are explained in the caption of Fig.(2).

we show the transversely distorted density of unpolarized quarks in a nucleon with spin in x-direction (coming from the dipole-term $\propto \epsilon^{ji} b_\perp^j S_\perp^i$ in Eq. (9)), which has already been discussed in [21]. A new observation is that the GPD $\overline{E}_T$ also leads to a strong transverse distortion orthogonal to the transverse quark spin for an *unpolarized* nucleon (coming from the dipole-term $\propto \epsilon^{ji} b_\perp^j s_\perp^i$ in Eq. (9)) on the RHS of Fig.(2). It was argued in [9] that this shift in $+y$-direction[b] may correspond to a non-zero, negative Boer-Mulders function [22] $h_1^\perp < 0$ for up-quarks. The distortions due to transverse quark and nucleon spin add up for the density on the LHS in Fig.(3), while it goes in opposite $(-y)$-direction for quarks with spin opposite to the nucleon spin, as can be seen on the RHS of Fig.(3). Interestingly, there is practically no influence visible from the quadrupole-term $\propto s_\perp^i (2b_\perp^i b_\perp^j - b_\perp^2 \delta^{ij}) S_\perp^j$ in Eq. (9) for the up-quark densities.

4. Conclusions and outlook

Our lattice results for the transversity distribution suggests that the Soffer bound is saturated by $\approx 60 - 80\%$ for the lowest two x-moments. In addition, we have presented preliminary results for the lowest moment of the transverse spin density of quarks in the nucleon. The distortion of the density of transversely polarized quarks in an unpolarized nucleon is substantial and could give rise to a non-vanishing negative Boer-Mulders function for up-quarks through final state interactions as argued by Burkardt [9].

---

[b]or equivalently a shift in $(-x)$-direction for quarks with spin in y-direction

8

We plan to extend our analysis of transverse spin densities in lattice QCD to the lowest two moments of up- and down-quarks and to investigate improved positivity bounds for GPDs which have been obtained in [7].

Acknowledgments

References

1. D. Müller *et al.*, Fortsch. Phys. **42** (1994) 101 [hep-ph/9812448]; X. Ji, Phys. Rev. D **55** (1997) 7114 [hep-ph/9609381]; A. V. Radyushkin, Phys. Rev. D **56** (1997) 5524 [hep-ph/9704207].
2. M. Diehl, Phys. Rept. **388** (2003) 41 [hep-ph/0307382].
3. X. Ji, Phys. Rev. Lett. **78** (1997) 610 [hep-ph/9603249].
4. M. Burkardt, Phys. Rev. D **62** (2000) 071503 [Erratum-ibid. D **66** (2002) 119903] [hep-ph/0005108].
5. M. Diehl, Eur. Phys. J. C **25** (2002) 223 [Erratum-ibid. C **31** (2003) 277] [hep-ph/0205208].
6. Ph. Hägler *et al.*, Phys. Rev. Lett. **93** (2004) 112001 [hep-lat/0312014].
7. M. Diehl, Ph. Hägler, Eur. Phys. J. C **44** (2005) 87 [hep-ph/0504175].
8. M. Diehl, Eur. Phys. J. C **19** (2001) 485 [hep-ph/0101335].
9. M. Burkardt, hep-ph/0505189.
10. Ph. Hägler, Phys. Lett. B **594** (2004) 164 [hep-ph/0404138].
11. Z. Chen and X. Ji, Phys. Rev. D **71** (2005) 016003 [hep-ph/0404276].
12. M. Göckeler *et al.*, Phys. Rev. Lett. **92** (2004) 042002 [hep-ph/0304249].
13. Ph. Hägler *et al.*, Phys. Rev. D **68** (2003) 034505 [hep-lat/0304018].
14. M. Göckeler *et al.*, Phys. Lett. B **627** (2005) 113 [hep-lat/0507001].
15. G. Martinelli *et al.*, Nucl. Phys. B **445** (1995) 81 [hep-lat/9411010]; M. Göckeler *et al.*, Nucl. Phys. B **544** (1999) 699 [hep-lat/9807044].
16. M. Göckeler *et al.*, Few Body Syst. **36** (2005) 111 [hep-lat/0410023].
17. M. Göckeler *et al.*, Nucl. Phys. A **755** (2005) 537 [hep-lat/0501029].
18. J. Soffer, Phys. Rev. Lett. **74** (1995) 1292 [hep-ph/9409254]; D. W. Sivers, Phys. Rev. D **51** (1995) 4880.
19. G. Altarelli *et al.*, Nucl. Phys. B **534** (1998) 277 [hep-ph/9806345].
20. M. Göckeler *et al.*, *in preparation*.
21. M. Burkardt, Int. J. Mod. Phys. A **18** (2003) 173 [hep-ph/0207047].
22. D. Boer, P. J. Mulders, Phys. Rev. D **57** (1998) 5780 [hep-ph/9711485].
23. C. R. Allton *et al.*, Phys. Rev. D **65** (2002) 054502 [hep-lat/0107021].